(Preprint) AAS 18-384

INCREMENTAL STATES FOR PRECISE ON-ORBIT RELATIVE KNOWLEDGE IN FORMATION FLIGHT

Martin Cacan,* Andrew Harris,† Jack Aldrich,* David Bayard,* Carl Seubert,*

High precision and close proximity formation flight is an enabling technology for future space missions and requires an on-board relative navigation capability that is accurate to the mm-level and robust to formation parameters. Common estimation techniques linearize the entire formation about one spacecraft's position, resulting in degraded accuracy due to linearization errors when separation distances become large. Additionally, methods which decouple absolute and relative state estimates usually require ad-hoc methods to incorporate the estimates together. This work discusses an alternative "incremental" formulation of the relative navigation problem which is invariant to formation size, robust to coupling between absolute and relative dynamics, and can undergo similarity transformations to smoothly incorporate either absolute or relative information without numerical issues. A specific example of this architecture is presented in the context of formation navigation using Carrier-Differential Global Positioning System measurements, and is compared to a traditional leader-linearized filter. In the presence of accurate measurements, the incremental architecture is shown to reduce linearization errors and mean estimate errors by up to three orders of magnitude without the incorporation of new sensor information.

INTRODUCTION

Formations of small satellites have the potential to replace monolithic structures due to their low cost, versatility, and ability to form a distributed sensor network. For this application, new science missions have been proposed which require tight formations (m-level separation) with accurate control (mm-level) that is fuel-efficient for multi-year missions. One of the key components to controlling the relative position to the mm-level and improving fuel efficiency is through accurate estimation. In particular, relative velocity estimation errors are the largest contributor to excess fuel consumption.[1] Simple attempts to reduce fuel usage by tuning control deadbands to minimize thruster pulsing can have the opposite effect in the presence of knowledge error and act to drive up fuel consumption and degrade control performance.

Real-time relative estimation strategies presented in the literature vary from differenced absolute estimates[6,14] to estimation of only the relative state by assuming the leader position is known.[2,3] Individually estimating and controlling a set of spacecraft based on prescribed relative positions is often sufficient when high-precision is not required, such as the TerraSAR-X to TanDEM-X formation in "single-spacecraft" mode.[8] This class of systems is separately classified as a constellation, following the convention of Scharf et al.[11] Relative only estimation, often leveraging the linearized

*Guidance, Navigation, and Controls Engineer, Autonomous Systems Division, Jet Propulsion Laboratory, California Institute of Technology. 4800 Oak Grove Drive Pasadena CA 91109.

†Guidance, Navigation, and Controls Engineering Intern, Autonomous Systems Division, Jet Propulsion Laboratory, California Institute of Technology. 4800 Oak Grove Drive Pasadena CA 91109.

Hill-Clohessy-Wiltshire (HCW) relative dynamics, is commonly used in rendezvous and docking as the primary vehicle is often running an independent estimator or ground based orbit determination to estimate its position.

The approximation of HCW dynamics for Guidance, Navigation, and Control (GNC) is not applicable to multi-year missions as fuel is spent driving the true dynamics to the linearized dynamics. Even when the true, nonlinear dynamics are considered, using the relative dynamics only formulation often linearizes the formation about the known leader. This leads to degraded performance at large baseline separation distances. Additionally, the coupling between the leader uncertainty and relative position uncertainty cannot be handled elegantly. This often results in uncertainty from the leader being pushed into the follower spacecraft.

This work discusses a navigation architecture which allows the user to control (and minimize) the linearizion error and improves the conditioning of the covariance matrix by introducing an optimal state transform. The navigation algorithm must only estimate the very small "incremental states" (incremental = actual minus nominal), where the nominal values are carefully constructed from guidance and prior estimates. This resolves the issue associated with linearizing the formation about the leader, as each spacecraft can be linearized about itself. The performance of the proposed algorithm in this work is completely insensitive to the size of the "leader-follower" separation baseline. This is an important and versatile feature of this work as it is applicable to a large range of future science missions at Earth and beyond.

This paper is not the first to address the importance of estimating the incremental states as "deviations from a known nearby reference". GPS observables are more accurately characterized in terms of the incremental state covariances, not the full state covariances.[12] Likewise, position state estimate propagation is frequently handled kinematically by using an incremental state formulation.[13] In a related field of attitude estimation, the notion of known nominals and the associated incremental state estimation problem is immediately obvious. For example, the multiplicative extended Kalman filter, known as MEKF in the attitude quaternion estimation literature, propagates the *small* incremental states which can be considered linear through the small angle approximation.[4,7,10,16]

Most importantly, the concept of the incremental state is the heart of what makes the extended Kalman filter (EKF) a powerful tool. The EKF selects the *nominal* as the most recent estimate, and linearizes the system about this point to estimate the incremental deviation away from the nominal. However, it is the point of this paper to highlight the ways in which controlling the linearization process through incremental states prior to application of the filter can improve the filter numerics and reduce the divergence between *nonlinear* state and *linear* covariance propagation. Additionally, when explicitly posing the state dynamics in the incremental form, the state and Kalman filter itself can be transformed to elegantly handle updates of the absolute or relative positions depending on the form of the measurement.

The remainder of the paper is organized as follows. The incremental Kalman filtering approach is presented next in a general form for application to a wide variety of nonlinear problems. After, the paper focuses on the formation flying estimation problem by presenting the single and relative orbital dynamics. The incremental architecture is then applied to this problem to estimate both the leader, follower, and relative positions. Extensive results of the method are presented for varying update rates and baseline separation distances. In addition, results of a more traditional 'relative only' estimation algorithm are presented for comparison. A summary of the work and key conclusions are presented at the end.

INCREMENTAL ESTIMATION ARCHITECTURE

Continuous-Time Incremental Dynamics

Consider the continuous-time nonlinear plant model that is affine in control.

$$\begin{aligned} \dot{x} &= f(x,t) + B(t)u + L(t)w \\ y &= h(x,t) + M(t)v \end{aligned} \tag{1}$$

Here, the state $x \in \mathbb{R}^{n_x}$, the control input $u \in \mathbb{R}^{n_u}$, the process noise $w \in \mathbb{R}^{n_w}$, and output noise $v \in \mathbb{R}^{n_v}$ satisfy

$$u = u_o + u_s, \quad w = w_o + w_s, \quad v = v_o + v_s \tag{2}$$

where the *nominal* control input u_o, process noise w_o, and output noise v_o are known by assumption, and may be arbitrary, finite, and time-varying in the most general setting. The *incremental* control input $u_s(t)$, process noise $w_s(t)$, and output noise $v_s(t)$ are zero-mean Gaussian noise processes with covariances given by:

$$\begin{aligned} E[u_s(t)u_s(\tau)^T] &= P_{uu}\delta(t-\tau), & E[w_s(t)u_s(\tau)^T] &= P_{wu}\delta(t-\tau) \\ E[w_s(t)w_s(\tau)^T] &= P_{ww}\delta(t-\tau), & E[w_s(t)v_s(\tau)^T] &= 0 \\ E[v_s(t)v_s(\tau)^T] &= P_{vv}\delta(t-\tau), & E[u_s(t)v_s(\tau)^T] &= 0 \end{aligned} \tag{3}$$

Consider the change-of-variables using Equation (2) and the *nominal* state and output vectors, x_o and y_o, respectively.

$$\begin{aligned} x_s &= x - x_o & u_s &= u - u_o \\ y_s &= y - y_o & w_s &= w - w_o \\ & & v_s &= v - v_o \end{aligned} \tag{4}$$

Here, it is assumed that the *nominal* variables $\{x_o, u_o, w_o, y_o, v_o\}$ are known while the *true* variables $\{x, u, w, y, v\}$ are unknown and must be estimated using the incremental variables.

Because the nominal variables are known, the *nominal process information*,

$$f(x_o,t) \triangleq \left[f(x,t) \right]_{x=x_o(t)}, \qquad A(t) \triangleq \left[\frac{\partial f(x,t)}{\partial x} \right]_{x=x_o(t)}$$

and the *nominal output information*,

$$h(x_o,t) \triangleq \left[h(x,t) \right]_{x=x_o(t)}, \qquad C(t) = \left[\frac{\partial h(x,t)}{\partial x} \right]_{x=x_o(t)}$$

are known in terms of the model functionals, $f(\cdot)$ and $h(\cdot)$, which are assumed to be known *exactly*.

Most importantly, (1) is *exactly* equivalent to

$$\begin{aligned} \dot{x} &= f(x_o,t) + A(t)x_s + B(t)(u_s + u_o) + L(t)(w_s + w_o) + f_e(x_s,t) \\ y &= h(x_o,t) + C(t)x_s + M(t)(v_s + v_o) + h_e(x_s,t) \end{aligned} \tag{5}$$

for any choice of nominals. Model linearization error is captured by $f_e(\cdot)$ and $h_e(\cdot)$ which are small when the scale of the states being estimated is also small. This provides motivation for the use of incremental states which are small by design.

From the change-of-variables (4), taking the time-derivative of $x_s = x - x_o$ yields $\dot{x}_s = \dot{x} - \dot{x}_o$, and therefore, the *incremental* system dynamics are governed by

$$\begin{aligned} \dot{x}_s &= \dot{x} - \dot{x}_o \\ y_s &= y - y_o \end{aligned} \tag{6}$$

where the nominal dynamics are governed by the unperturbed nonlinear system.

$$\begin{aligned} \dot{x}_o &= f(x_o,t) + B(t)u_o + L(t)w_o \\ y_o &= h(x_o,t) + M(t)v_o \end{aligned} \tag{7}$$

Substituting Equations (5) and (7) into Equation (6) yields the incremental dynamic system.

$$\begin{aligned} \dot{x}_s &= A(t)x_s + B(t)u_s + L(t)w_s + f_e(x_s,t) \\ y_s &= C(t)x_s + M(t)v_s + h_e(x_s,t) \end{aligned}$$

Equivalently, the incremental dynamics become

$$\begin{aligned} \dot{x}_s &= A(t)x_s + w_r \\ y_s &= C(t)x_s + v_r \end{aligned} \tag{8}$$

where w_r is the *resultant* process noise, and v_r is the *resultant* output/measurement noise given by

$$\begin{aligned} w_r &\triangleq B(t)u_s + L(t)w_s + f_e(x_s,t) \\ v_r &\triangleq M(t)v_s + h_e(x_s,t) \end{aligned} \tag{9}$$

Kalman Filtering of the Incremental System

Assume that the *incremental* system (8), which includes nonlinearities, is approximated by the linear, time-varying (LTV) stochastic system,

$$\begin{aligned} \dot{x}_s &= A(t)x_s + w_r \qquad & E[w_r(t)w_r(\tau)^T] &= Q(t)\delta(t-\tau) \\ y_s &= C(t)x_s + v_r \qquad & E[v_r(t)v_r(\tau)^T] &= R(t)\delta(t-\tau) \end{aligned} \tag{10}$$

and the perturbations w_r and v_r are approximated by zero-mean white noise processes with covariances Q and R given by

$$\begin{aligned} Q &= BP_{uu}B^T + LP_{ww}L^T + P_{f,e} \\ R &= MP_{vv}M^T + P_{h,e} \end{aligned}$$

Here, $P_{f,e}$ and $P_{h,e}$ represent positive-definite uncertainty matrices associated with process and output modeling error from linearization and unmodeled effects. It is easy to see that the these nonlinearities need to be kept small because they negatively impact estimator uncertainty. In other words, these covariances are reduced when the nonlinearity itself if reduced.

Given (10), the continuous-time Kalman Filter of the incremental state becomes:

$$\begin{aligned} \dot{\hat{x}}_s &= A\hat{x}_s + K(y_s - C\hat{x}_s) \\ \dot{P} &= AP + PA^T - PC^T R^{-1} CP + Q \\ \hat{x}_s(0) &= E[x_s(0)] = 0, \qquad K = PC^T R^{-1} \\ P(0) &= E[\{x_s(0) - \hat{x}_s(0)\}\{x_s(0) - \hat{x}_s(0)\}^T] \end{aligned} \tag{11}$$

where explicit time dependence, $P = P(t)$, $Q = Q(t)$, $R = R(t)$, $A = A(t)$, $C = C(t)$ and $K = K(t)$ is assumed. The original state estimate $\hat{x}$ is computed by summing the nominal state x_o with the incremental state estimate $\hat{x}_s$ as

$$\hat{x} = x_o + \hat{x}_s$$

Note that Algorithm (11) is actually the continuous-time Linearized Kalman Filter (LKF).[5] Additionally, the exact system described by Equation (1) can be estimated using a continuous-time Extended Kalman Filter (EKF) which provides a simplified framework to reach the incremental state. In the EFK, the nominal is set as the previous estimate and generally abstracts away the concept of both the nominal and incremental states. As a result, the stability of the EKF is difficult to prove due to the feedback of state information and the fact that performance degrades as estimates degrade. Finally, the propagation of the dynamic equations can include known linearization errors $f_e(x_s,t)$ for improved propagation accuracy in either the LKF or EKF. The drawback is divergence of the state and covariance propagation, as the latter must be propagated linearly.

ORBITAL DYNAMICS

Let $n_{sc} \in \{2,3,4,...\}$ be the total number of spacecraft in the formation. Let $\mathcal{F} \coloneqq \{1,2,3,\ldots,n_{sc}\}$ be the set of formation flying spacecraft identification numbers such that each agent is distinguished from the others by its own ID. We define agent(1) as the formation *Leader* while agents($2\ldots n_{sc}$) are considered *Follower* spacecraft. Let $r_i \in \mathbb{R}^3$ be the position of agent(i) expressed in the Earth Centered Inertial (ECI) reference frame. Let $u_i \in \mathbb{R}^3$ be the control input of agent(i) expressed in ECI frame. Let $w_i \in \mathbb{R}^3$ be the disturbance input of agent(i) expressed in ECI frame. This term is a disturbing force attributed to non-spherical Earth, third body gravity, aerodynamic drag, solar radiation pressure, and any errors attributed to unmodeled effects. As such, the dynamics of a single satellite around a primary body with an associated output function can be expressed generally as:

$$\begin{aligned} \ddot{r}_i &= g(r_i) + u_i + w_i \qquad \forall i \in \mathcal{F} \\ y_i &= h(r_i) + v_i \end{aligned} \tag{12}$$

where $g(r)$ is a generalized vector-valued gravity function and $h(r)$ is the measurement function. For example, when an inverse square-law gravity potential is assumed, $g(r)$ becomes

$$g(r) = -\mu \frac{r}{\|r\|^3} \tag{13}$$

Incremental Dynamics

Consider the following change-of-variables to the incremental state, also shown graphically for a formation of $n_{sc} = 2$ in Figure 1.

$$r_i = \tilde{r}_i + \delta_i \qquad \forall i \in \mathcal{F}$$

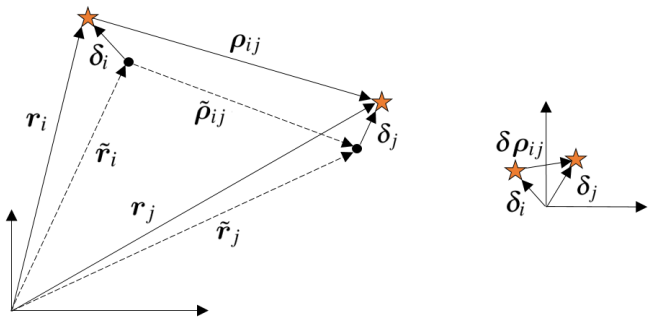

Figure 1: Geometric representation of incremental states.

The absolute position r_i of agent(i) is separated into the nominal position $\tilde{r}_i$, and the incremental position δ_i. The nominal dynamics are governed by

$$\ddot{\tilde{r}}_i = g(\tilde{r}_i) \qquad \forall i \in \mathcal{F} \tag{14}$$

Observe that $\ddot{\delta}_i = \ddot{r}_i - \ddot{\tilde{r}}_i$, which upon substitution of (12) and (14) yields

$$\ddot{\delta}_i = d(\tilde{r}_i, \delta_i) + u_i + w_i \qquad \forall i \in \mathcal{F} \tag{15}$$

where the gravitational drift term $d(\cdot,\cdot)$ is defined as

$$d(\tilde{r}_i, \delta_i) \triangleq g(\tilde{r}_i + \delta_i) - g(\tilde{r}_i) \qquad \forall i \in \mathcal{F}$$

Let the gravity gradient be defined as

$$G(r) \triangleq \frac{\partial g(r)}{\partial r} \tag{16}$$

which for the inverse square law gravity vector (13) becomes

$$G(r) = \frac{\mu}{\|r\|^5}\left(3rr^T - \|r\|^2 I\right)$$

Using (16), it is easy to express (15) as

$$\ddot{\delta}_i = G(\tilde{r}_i)\delta_i + u_i + w_i + d_e(\tilde{r}_i, \delta_i) \qquad \forall i \in \mathcal{F} \tag{17}$$

where $d_e(\tilde{r}_i, \delta_i)$ is the linearization error given by

$$d_e(\tilde{r}_i, \delta_i) \triangleq d(\tilde{r}_i, \delta_i) - G(\tilde{r}_i)\delta_i \qquad \forall i \in \mathcal{F}$$

Neglecting the nonlinearity, observe that (17) can be expressed in first order form as

$$\dot{z}_i = \Gamma(\tilde{r}_i) z_i + \Lambda(u_i + w_i) \qquad \forall i \in \mathcal{F} \tag{18}$$

where state z_i, state transition $\Gamma(\cdot)$, and control influence map Λ are

$$z_i \triangleq \begin{bmatrix} \delta_i \\ \dot{\delta}_i \end{bmatrix}, \qquad \Gamma(\tilde{r}_i) \triangleq \begin{bmatrix} 0 & I \\ G(\tilde{r}_i) & 0 \end{bmatrix}, \qquad \Lambda \triangleq \begin{bmatrix} 0 \\ I \end{bmatrix}$$

The accompanying output function (12) can also be linearized about the output of the nominal state to yield the incremental output function.

$$y_i = h(\tilde{r}_i, t) + \frac{\partial h}{\partial r_i}\Big|_{r_i=\tilde{r}_i}(r_i - \tilde{r}_i) + v_i \tag{19}$$

$$\delta y_i = \Theta(\tilde{r}_i) z_i + v_i \tag{20}$$

where $y_i = \tilde{y}_i + \delta y_i$. In this first order LTV incremental form, the nonlinearities are minimized by ensuring the state z_i is small as each spacecraft is linearized about its own nominal value instead of the *Leader* spacecraft.

Change of Basis: Absolute and Relative Dynamics

When a formation is considered, the states of each spacecraft can be concatenated, $z = [z_1 \dots z_{n_{sc}}]^T$ which describes the absolute incremental position of each spacecraft in $\mathcal{F}$. The LTV dynamics of the full formation can clearly be represented in the incremental form of Equation (8). For example, consider the case of three spacecraft flying in formation. Then $n_{sc} = 3$, and the leader/follower relative dynamics become

$$\begin{aligned} \dot{z} &= \mathcal{A}(\tilde{r}_1, \tilde{r}_2, \tilde{r}_3) z + \mathcal{B} u + \mathcal{B} w \\ y &= \mathcal{C}(\tilde{r}_1, \tilde{r}_2, \tilde{r}_3) z \end{aligned} \tag{21}$$

where nominal position vectors are inherently a function of time. The vectors $\{z, u, w, v\}$ and matrix-valued functions $\{\mathcal{A}, \mathcal{B}, \mathcal{C}\}$ are defined as

$$z \triangleq \begin{bmatrix} z_1 \\ z_2 \\ z_3 \end{bmatrix}, \qquad u \triangleq \begin{bmatrix} u_1 \\ u_2 \\ u_3 \end{bmatrix}, \qquad w \triangleq \begin{bmatrix} w_1 \\ w_2 \\ w_3 \end{bmatrix}$$

$$\mathcal{A} \triangleq \begin{bmatrix} \Gamma(\tilde{r}_1) & 0 & 0 \\ 0 & \Gamma(\tilde{r}_2) & 0 \\ 0 & 0 & \Gamma(\tilde{r}_3) \end{bmatrix}, \qquad \mathcal{B} \triangleq \begin{bmatrix} \Lambda & 0 & 0 \\ 0 & \Lambda & 0 \\ 0 & 0 & \Lambda \end{bmatrix}, \quad \mathcal{C} \triangleq \begin{bmatrix} \Theta(\tilde{r}_1) & 0 & 0 \\ 0 & \Theta(\tilde{r}_2) & 0 \\ 0 & 0 & \Theta(\tilde{r}_3) \end{bmatrix}$$

From the dynamical system and the output equations (21), the Kalman filter algorithm defined in Equation (11) can be applied to estimate the absolute positions. When provided absolute measurements, the output is equal to the state and $\mathcal{C}(t)$ is the identity matrix. When relative measurements are considered such as carrier-difference GPS or inter-satellite ranging, the measurement matrix $\mathcal{C}(t)$ can be chosen to subtract one state from another to output the relative state. In the example of three spacecraft, $\mathcal{C} = [-I \quad I \quad 0]$, where I is the identity matrix, produces a relative incremental output between the first two spacecraft. However, it is noted that there are often numerical issues with this formulation as the conditioning of the covariance matrix degrades given *precise* relative measurements. As a result, it is often best to chose states of the filter that are directly measured to improve performance.

Instead of modifying $\mathcal{C}$, it is best to modify the state and dynamics using a similarity transform. Consider the following similarity transformation:

$$x = Tz, \quad A = T\mathcal{A}T^{-1}, \quad B = T\mathcal{B}, \quad C = \mathcal{C}T^{-1} \tag{22}$$

which transforms (21) into a relative dynamic form.

$$\begin{aligned} \dot{x} &= A(t)x + Bu + Bw \\ y &= C(t)x + v \end{aligned} \tag{23}$$

Here, T is selected by hand to convert two of the filter states from absolute to relative states. Note, the choice of T is limited to invertible matrices.

$$T = \begin{bmatrix} I & 0 & 0 \\ -I & I & 0 \\ -I & 0 & I \end{bmatrix}, \quad x = Tz = \begin{bmatrix} z_1 \\ z_2 - z_1 \\ z_3 - z_1 \end{bmatrix}$$

Here, x_1 acts as the absolute reference for the formation and $\{x_2, x_3\}$ describe the small, relative displacement error, represented by $\{\delta\rho_{12}, \delta\rho_{13}\}$ based on Figure 1. Note, another transformation could have be chosen to yield a state describing $\delta\rho_{23}$. It is important to note that x is still an *incremental* variable in that it is with respect to the nominal relative position. As such, linearization errors remain small even when baseline separation distance of the formation increases.

Additionally, note that this transformation results in the new state transition matrix that has a direct coupling between the absolute and relative states:

$$A(t) = \begin{bmatrix} \Gamma(\tilde{r}_1) & 0 & 0 \\ \Gamma(\tilde{r}_2) - \Gamma(\tilde{r}_1) & \Gamma(\tilde{r}_2) & 0 \\ \Gamma(\tilde{r}_3) - \Gamma(\tilde{r}_1) & 0 & \Gamma(\tilde{r}_3) \end{bmatrix} \tag{24}$$

Finally, it is important to note that the similarity transform can be applied at any intermediate step in the filtering process as long as the transformation is also applied to Kalman filter matrices $\{P, Q, R\}$. This is crucial for accurately folding in both absolute and relative measurements. Given a formation where each spacecraft is equipped with both GPS receiver and inter-spacecraft ranging device, the state of the filter can be transformed between sequential updates of the Kalman filter at the same time step. This allows both absolute and relative measurements to be incorporated into the filter with improved numerics as the measurement is always of the state being estimated. The combination of the incremental linearization process and similarity transform provides a useful way to incorporate a wide set of measurements and estimate a variety of similar states.

FORMATION ESTIMATION USING CARRIER-DIFFERENTIAL GPS

This section details how the incremental Kalman filtering approach is applied to the spacecraft formation estimation problem with the goal of achieving highly-accurate relative position estimation using Carrier-Differential GPS (CDGPS). For simplicity, the initial example of two spacecraft represented by agent(i) and agent(j) is considered. The same similarity transformation can be applied to change the absolute incremental state vector into the relative incremental state.

$$\boldsymbol{z} = \begin{bmatrix} \boldsymbol{\delta}_i \\ \dot{\boldsymbol{\delta}}_i \\ \boldsymbol{\delta}_j \\ \dot{\boldsymbol{\delta}}_j \end{bmatrix}, \quad \boldsymbol{x} = \begin{bmatrix} \boldsymbol{\delta}_i \\ \dot{\boldsymbol{\delta}}_i \\ \boldsymbol{\delta}_j - \boldsymbol{\delta}_i \\ \dot{\boldsymbol{\delta}}_j - \dot{\boldsymbol{\delta}}_i \end{bmatrix} \triangleq \begin{bmatrix} \boldsymbol{\delta}_i \\ \dot{\boldsymbol{\delta}}_i \\ \boldsymbol{\delta\rho}_{ij} \\ \dot{\boldsymbol{\delta\rho}}_{ij} \end{bmatrix}, \quad \tilde{x} = \begin{bmatrix} \tilde{r}_i \\ \dot{\tilde{r}}_i \\ \tilde{\rho}_{ij} \\ \dot{\tilde{\rho}}_{ij} \end{bmatrix} \tag{25}$$

The second order dynamics associated with the relative state vector ρ_{ij} can be found be differencing Equation (12). For an inverse-square gravity, the relative dynamics can be defined as:

$$\ddot{\boldsymbol{\rho}}_{ij} = \frac{\mu}{||r_i||^3}\left[\boldsymbol{r}_i - \frac{||r_i||^3(\boldsymbol{r}_i+\boldsymbol{\rho}_{ij})}{||(\boldsymbol{r}_i+\boldsymbol{\rho}_{ij})||^3}\right] + \Delta\boldsymbol{u}_D^{ij} + \Delta\boldsymbol{u}_C^{ij} \tag{26}$$

where $\Delta\boldsymbol{u}_{D(C)}^{ij}$ represents the differential disturbing (control) forces. Equation (26) can be converted into the incremental domain following the same procedure outlined in the previous section. In this case, the incremental relative position is taken with respect to the nominal separation, i.e. $\rho = \tilde{\rho} + \delta\rho$. Notably, these dynamics are directly dependent on knowledge of the absolute position of the leader spacecraft. The use of δ_i states on the absolute position enables this filter to estimate the true contributions to the relative motion from displacements on both the absolute and relative states; in comparison, formulations which decouple the absolute and relative estimation attribute all motion of the relative dynamics as the motion of only the *Follower* spacecraft.

As a note, it can be shown that the incremental absolute dynamics δ_i defined in Equation (15) are exactly equal to (26) when the vectors $\{r_i, \rho_{ij}\}$ are replaced with $\{\tilde{r}_i, \delta_i\}$. This makes sense as the incremental absolute dynamics of agent(i) are just the relative motion of the spacecraft with respect to the nominal spacecraft location.

As a comparator, an estimator was designed based on the more conventional approach which decouples the absolute and relative estimation.[3,6,8] This filter is described as a "Leader-Linearized" extended Kalman filter or LL-EKF in the text; the incremental approach outlined in this work is described as an incremental Kalman Filter or I-KF for the remainder of this work. By assuming the position of the leader is known, Equation (26) completely describes the nonlinear relative dynamics. An estimate of $\boldsymbol{\rho}_{ij}$ can be generated by implementing an EKF, centered around the known leader position $\boldsymbol{r}_i$. This section provides a comparison between the methods with a focus on benefits of the incremental architecture.

Incremental Measurement Equations

A transformation of the nonlinear measurement equations into the incremental domain must be completed to provide an incremental measurement (with respect to the nominal) to the Kalman filter. For clarity, a derivation of the CDGPS-specific incremental measurement function is presented here. Typically, the use of CDGPS in real applications requires the estimation of additional GPS-specific parameters that are not related to the architecture-focused arguments of this paper. For example, the impact of clock and transmitter biases is potentially large for real applications; however, such effects will impact both filters approximately evenly. Instead, the focus of this analysis is on the performance differences due strictly to the nonlinear measurement model and dynamics, which couple the relative and absolute state dynamics.

For the absolute GPS ranging case, a simple "range-plus-noise" model is used for the observed phases from the kth GPS satellite:

$$\phi_i^k = ||\boldsymbol{r}_{GPS}^k - \boldsymbol{r}_i|| + w_\phi^k = ||\boldsymbol{r}_{GPS}^k - (\tilde{\boldsymbol{r}}_i + \boldsymbol{\delta}_i)|| + w_\phi^k \tag{27}$$

For a pair of satellites, the differential phase observed is therefore modeled as

$$\Delta\phi_{ij}^k = ||\boldsymbol{r}_{GPS}^k - \boldsymbol{r}_i|| - ||\boldsymbol{r}_{GPS}^k - \boldsymbol{r}_j|| + w_{\Delta\phi}^k \tag{28}$$

where $w^k_{\Delta\phi}$ is the noise associated with that signal. Substituting in the expression for $\boldsymbol{r}_j$ in terms of $\boldsymbol{\rho}_{ij}$ yields:

$$\Delta\phi^k_{ij} = ||\boldsymbol{r}^k_{GPS} - \boldsymbol{r}_i|| - ||\boldsymbol{r}^k_{GPS} - (\boldsymbol{r}_i + \boldsymbol{\rho}_{ij})|| + w^k_{\Delta\phi} \tag{29}$$

Notably, this expression of a *relative* position measurement is dependent on the *absolute* position of the i^{th} spacecraft in addition to the relative state. Once again, the presence of the absolute states in this expression couples the absolute and relative states, and results in inconsistencies when the absolute states are ignored.

This nonlinear measurement function is linearized about the nominal expected measurement by differencing the expected and corrected measurement functions:

$$h(x) = h(\tilde{\boldsymbol{x}} + \boldsymbol{x}) - h(\tilde{\boldsymbol{x}}) \tag{30}$$

Re-writing this in terms of the incremental states $\boldsymbol{\delta}_i$ and $\delta\boldsymbol{\rho}_{ij}$ yields

$$\Delta\tilde{\phi}^k_{ij} = ||\boldsymbol{r}^k_{GPS} - (\tilde{\boldsymbol{r}}_i)|| - ||\boldsymbol{r}^k_{GPS} - (\tilde{\boldsymbol{r}}_i + \tilde{\boldsymbol{\rho}}_{ij})|| + w^k_{\Delta\phi} \tag{31}$$

$$\Delta\phi^k_{ij} = ||(\boldsymbol{r}^k_{GPS} - \tilde{\boldsymbol{r}}_i) - \boldsymbol{\delta}_i|| - ||(\boldsymbol{r}^k_{GPS} - \tilde{\boldsymbol{r}}_i - \boldsymbol{\delta}_i - \tilde{\boldsymbol{\rho}}_{ij}) - \boldsymbol{\delta}\boldsymbol{\rho}_{ij})|| + w^k_{\Delta\phi} \tag{32}$$

To use this formulation in a Kalman filter, it is required to take partials of this measurement equation with respect to the incremental states. In this sense, the measurement model is linearized about the expected nominal measurement:

$$\delta\Delta\phi^k_{ij} = \Delta\phi^k_{ij}(x) - \Delta\phi^k_{ij}(\tilde{x}) \tag{33}$$

Additionally, we note the definition of the derivative of a differential 2-norm with respect to a vector in it as given by the Matrix Cookbook:

$$\frac{\partial}{\partial \boldsymbol{x}}||\boldsymbol{x} - \boldsymbol{a}|| = \frac{\boldsymbol{x} - \boldsymbol{a}}{||\boldsymbol{x} - \boldsymbol{a}||} \tag{34}$$

which is simply the unit vector from $\boldsymbol{a}$ to $\boldsymbol{x}$ (otherwise referred to as the "line-of-sight" (LOS^x_a) vector). Next, we apply this to the set of states to yield the following non-zero partials:

$$\frac{\partial\Delta\phi^k_{ij}}{\partial\boldsymbol{\delta}_i} = -\frac{\boldsymbol{\delta}_i - (\boldsymbol{r}^k_{GPS} - \tilde{\boldsymbol{r}}_i)}{||\boldsymbol{\delta}_i + (\boldsymbol{r}^k_{GPS} + \tilde{\boldsymbol{r}}_i)||} - \frac{(\boldsymbol{r}^k_{GPS} - \tilde{\boldsymbol{r}}_i - \tilde{\boldsymbol{\rho}}_{ij}) - \boldsymbol{\delta}\boldsymbol{\rho}_{ij})}{||(\boldsymbol{r}^k_{GPS} - \tilde{\boldsymbol{r}}_i - \tilde{\boldsymbol{\rho}}_{ij}) - \boldsymbol{\delta}\boldsymbol{\rho}_{ij})||} = \text{LOS}^k_i - \text{LOS}^k_j \tag{35}$$

$$\frac{\partial\Delta\phi^k_{ij}}{\partial\boldsymbol{\delta}\boldsymbol{\rho}_{ij}} = -\frac{(\boldsymbol{r}^k_{GPS} - \tilde{\boldsymbol{r}}_i - \tilde{\boldsymbol{\rho}}_{ij}) - \boldsymbol{\delta}\boldsymbol{\rho}_{ij})}{||(\boldsymbol{r}^k_{GPS} - \tilde{\boldsymbol{r}}_i - \tilde{\boldsymbol{\rho}}_{ij}) - \boldsymbol{\delta}\boldsymbol{\rho}_{ij})||} = \text{LOS}^k_i \tag{36}$$

These are combined into the matrix of measurement function partials for $k = 1 \ldots N$ CDGPS measurements as:

$$H_\Delta = \begin{bmatrix}(\text{LOS}_i - \text{LOS}_j) & \boldsymbol{0}_{N\times 3} & \text{LOS}_j & \boldsymbol{0}_{N\times 3}\end{bmatrix} \tag{37}$$

Likewise, the measurement partials for the absolute state are computed as:

$$H_{\text{abs}} = \begin{bmatrix}\text{LOS}_i & \boldsymbol{0}_{N\times 9}\end{bmatrix} \tag{38}$$

Table 1: Simulation parameters of the lead spacecraft and noise models.

Parameter	Value
SMA	6,947 km
Eccentricity	0.01
Inclination	20°
RAAN	20°
Argument of Perigee	0.0°
True Anomaly	0.0 °

(a) Lead spacecraft orbital elements.

Parameter	Value
Q_r	0m
$Q_{\dot{r}}$	0m/s
R_ϕ	1×10^{-3}m
$R_{\delta\phi}$	1×10^{-6}m

(b) Noise coefficients used in simulation.

Simulation Parameters

To evaluate the effectiveness and benefits of the incremental architecture, the aforementioned filter was run over a set of various formation baselines and compared against the traditional EKF formulation. The "leader" spacecraft orbital elements can be found in Table 1a, while the relative offset $\tilde{\rho}_{12}$ of the follower spacecraft is only considered in the along-track, curvilinear direction. Per the previous discussion measurement uncertainty, these results do not consider the presence of ionospheric delays, clock drifts, or other accuracy-degrading effects found in real CDGPS applications; the numerical accuracies of the filters presented herein do not correspond to expected on-orbit accuracies. Additionally, the assumed sensor accuracies and filter noise tuning parameters are listed in Table 1b.

Finally, note that continuous-time formulations of the dynamics and estimation algorithms have been discussed, but discrete-time versions were implemented for all simulations in this paper. The filters were run with an update rate of 1 Hz.

Performance Metrics

To demonstrate the effects of both linearization and modeling error, the relative state estimates for both filters were characterized over a range of baselines and measurement noises. Characterization of filter performance is described in three components; the mean 2-norm of the state error calculated over time, the mean 2-norm of the measurement residual, and the mean 2-norm of the linearization error. Here, the mean position and velocity errors are defined in terms of the RMS position and velocity errors:

$$\text{Mean}\Big(||\boldsymbol{x}(i)-\hat{\boldsymbol{x}}(i)||_2\Big), \quad \forall i \in 1\dots T \tag{39}$$

The mean linearization error for filter states is given by the difference between the nonlinear propagation of the prior states and the value of the predicted states using the linearized state transition matrix:

$$\bar{f}_e = \text{Mean}\Big(||f(\tilde{\boldsymbol{x}}(i)+\boldsymbol{x}(i))-f(\tilde{\boldsymbol{x}}(i))-\Phi\boldsymbol{x}(i)||_2\Big), \quad \forall i \in 1\dots T \tag{40}$$

Likewise, the mean measurement linearization error is given by:

$$\bar{h}_e = \text{Mean}\Big(||h(\tilde{\boldsymbol{x}}(i)+\boldsymbol{x}(i)) - h(\tilde{\boldsymbol{x}}(i)) - H\boldsymbol{x}(i)||_2\Big), \quad \forall i \in 1\ldots T \tag{41}$$

These linearization errors represent the difference between the linearized dynamics, which are used to propagate the filter covariance matrix, versus the true dynamics which can be used during state propagation in the filter. Large linearization errors are associated with poor filter performance.[15]

Numerical Observability Analysis

The first step of any filter evaluation is to determine whether or not the states estimated by a filter are observable given the system dynamics and measurements. Many have attempted to define measures of observability for nonlinear systems. A conceptual benefit of the incremental state architecture is that the incremental state dynamics should remain "more linear" than leader-linearized architectures. However, the true nonlinear dynamics of the system are still re-linearized over time, yielding a time-varying linear system about the nominal states.

Observability of the states over a specified time horizon M can be found by using the *Information Matrix*:[5]

$$W_O = \sum_{i=1}^{M} \Phi(t_M,t_i)^T H^T R^{-1} H \Phi(t_M,t_i) \tag{42}$$

For observability, the eigenvalues of this matrix must be positively bounded above and below by finite numbers. Additionally, the rank of this matrix indicates the number of observable directions associated with the system. To analyze the observability of the presented I-KF algorithm, the information matrix was computed using the linearized state transition dynamics and measurement matrix at each time over two orbits for an incremental filter using only the relative CDGPS measurements and for a filter using both the CDGPS and absolute GPS measurements. At each time, the maximum and minimum eigenvalues of the respective information matrices was computed along with the matrix rank. These results are captured in Figure 2. Provided both absolute and relative measurements, the system is fully observable as is expected. Without absolute measurements, the filter states are not fully observable; however, there is limited observability of the absolute states are observable with only relative information. This result echoes the results of Psiaki, which found that relative position measurements under J2-perturbed gravity dynamics could yield full estimates of the absolute positions and velocities of both spacecraft. Our assumption of simple two-body, inverse-square gravity eliminates this observability for the same reasons as those mentioned by Psaiki.[9] In the orbit-element space, there is an infinite number of orbits with varying right ascensions that produce identical relative dynamics.

As a result of this analysis, the remaining numerical simulations are computed using a version of the I-KF that includes measurements of the absolute GPS phases to ensure full observability.

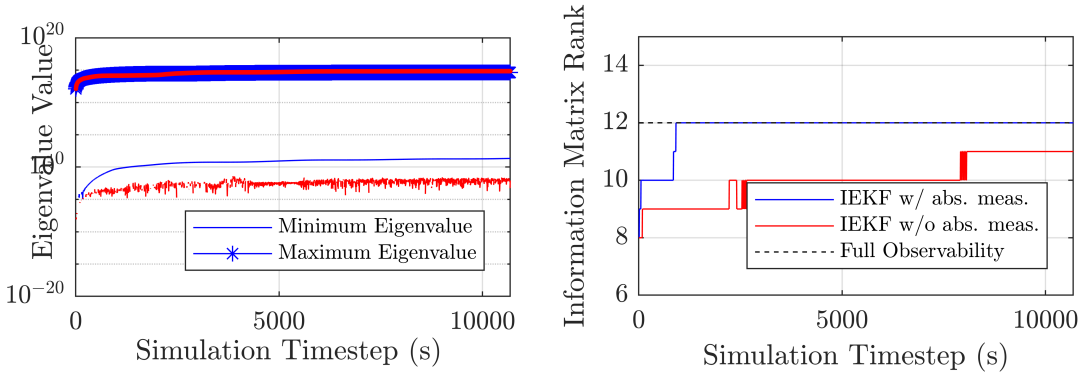

Figure 2: Evaluation of the Information Matrix properties as more measurements are combined. Red lines are for the filter run without absolute measurements, where the

Perfect Nominal Information

Minimizing the departure from nonlinearity and the size of states estimated by the filter is a key motivator behind the incremental architecture. To demonstrate this specific benefit of incrementalization, both the I-KF and the LL-KF are provided with ground truth as the nominal about which the dynamics are linearized; for the I-KF, this includes the ground truth of the follower spacecraft state. Under these conditions, estimation error is primarily driven by linearization error and model inaccuracy. To ensure that the results are comparable, both filters are provided with identical differential phase measurements with noises provided by Table 1b and initialized with identical states in the inertial frame.

A key underlying assumption behind the incremental linearization scheme is that the linearization error drives filter accuracy. However, this is primarily the case for filters using extremely accurate, precise measurements; when measurement noise is high, errors from linearization and departures from linearity are "washed out" by measurement noise. To demonstrate this effect, filter accuracy for position and velocity states is compared for various baselines and levels of measurement noise. Measurement noise levels are represented using the multiplier λ on the assumed variances listed in Table 1b. The results of this analysis for $\lambda = \{1, 10, 100, 1000\}$ are shown in Figure 3

Both filters feature similar relative positioning accuracies, which remain almost constant as the baseline grows and which scale log-linearly with increasing noise multipliers. This is consistent with the measurement model, which provides a direct estimate of the relative position for both filters. The impact of the incremental linearization is most apparent in the error behavior of the velocity states, which are inferred by each filter from the dynamics. The leader-linearized filter, which linearizes the follower velocity about the chief, sees its estimate accuracy degrade as the separation distance increases even with extremely high precision measurements. The incremental filter, on the other hand, remains sensitive to noise but is invariant to the baseline. Notably, the I-KF appears slightly more resistant to scaling with the quantity of measurement noise than the LL-KF. One explanation for this is the more precise velocity estimate provided by the I-KF's more consistent dynamical model, which allows the I-KF to weight its internal model more precisely than the LL-KF.

The performance metrics plotted in Figure 4 demonstrate the variation of linearization error in the

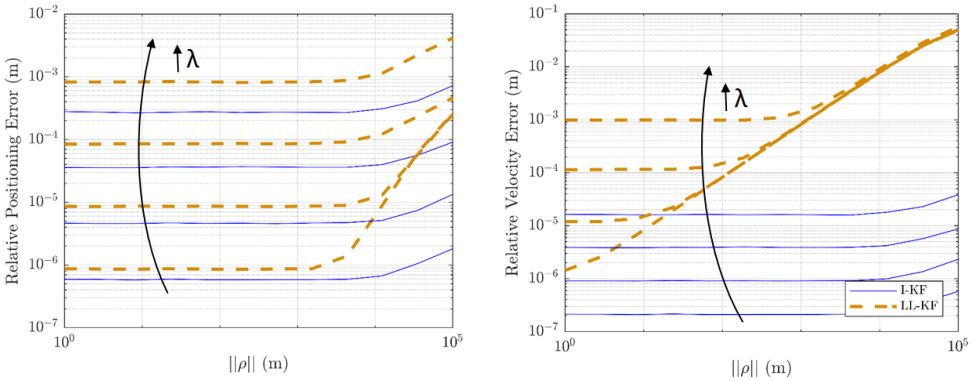

(a) Orbit-average RMS position error comparison. (b) Orbit-average RMS velocity error comparison

Figure 3: The I-KF (blue) provides superior minimization of both position and velocity linearization errors across all values of baseline separation and noise ($\lambda = \{1, 10, 100, 1000\}$) by up to an order of magnitude in comparison to the LL-KF (orange).

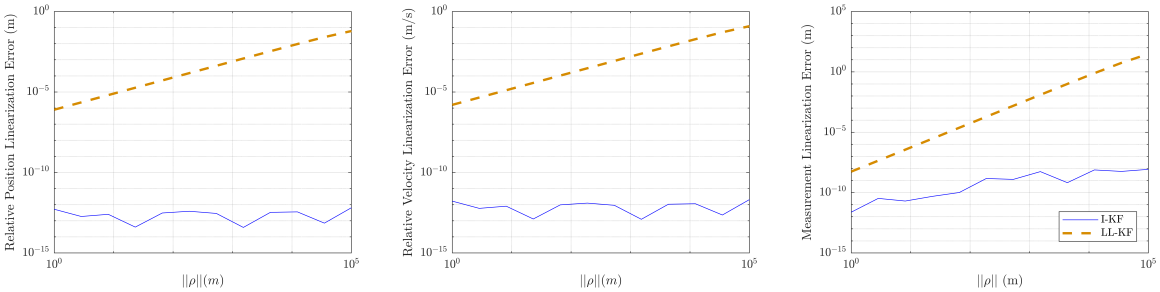

(a) Orbit-average RMS position linearization error comparison. (b) Orbit-average RMS velocity linearization error comparison (c) Orbit-average RMS measurement linearization error comparison.

Figure 4: Comparison of incremental (blue) and leader-linearized (orange) filter linearization errors with the formation baseline and level of measurement noise, with line-types representing different measurement noise levels. The I-KF linearization errors suffer from numerical instability due to their small magnitude.

position and velocity states for both filters as the baseline and level of measurement noise increases. Over all baselines, the leader-linearized filter suffers from substantially higher levels of linearization error in both its state and measurement models, whereas the incremental filter's small relative states result in extremely consistent linearizations and therefore small linearization errors. In all three cases, the I-KF experiences a lower level of both measurement and prediction linearization error while producing similar or better performance than the LL-KF.

The consistency of the incremental filter with respect to the true dynamics and measurement models is further demonstrated by evaluating the pre- and post-fit residuals, as shown in Figure 5 for a 1km baseline separation. In both cases, the incremental filter produces residuals that are zero-mean and normally distributed; by comparison, the residuals produced by the leader-linearized approach demonstrate both biases and dynamics as a result of the unacknowledged coupling between absolute

and relative states. These results drive the error dynamics shown in Figures 6 and 7, which demonstrate the time-history errors for the 10 kilometer baseline, $\lambda = 1{,}000$ case and their associated covariances.

The error trajectories for the leader-linearized filter clearly show evidence of the mis-modeled dynamics, and regularly push their 1-σ covariance bounds. At the same time, the incremental-linearized filter results show not only two to three orders of magnitude improvement in accuracy, but also tighter covariances in the relative states despite the large variances in the absolute δ_i states. This suggests two things: first, that the I-KF dynamics and measurement models more accurately capture the true behavior of the system; second, that the inclusion of coarsely-estimated absolute δ_i states does not adversely affect the accuracy of the $\delta\rho$ states.

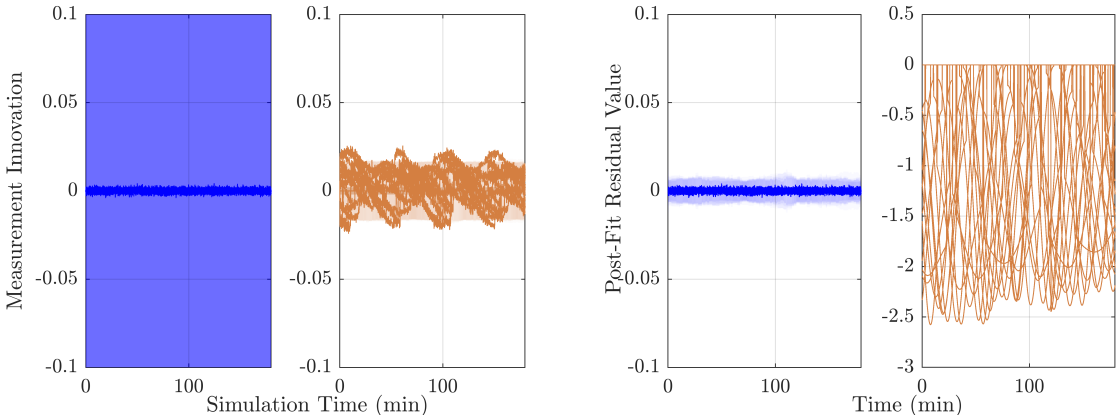

(a) Prefit residuals for both filters

(b) Post-fit residuals for both filters.

Figure 5: Post-fit measurement residuals for the I-KF (blue) and LL-KF (red) for ρ =10,000m, λ=1,000. Black lines indicate 1-σ covariance regions. Note that the LL-KF severely violates its pre- and post-fit covariance bounds due to model inconsistencies.

Imperfect Nominal Information

A major benefit of the incremental estimation architecture is the ability to compensate for dynamic mis-modeling due to errors in the leader inertial position. Here, the impact of mis-modeled nominal positions is evaluated by linearizing both filters about nearby two body orbits derived from randomly perturbing the initial position and velocity:

$$\tilde{\boldsymbol{r}}_i = \boldsymbol{r}_i + \kappa\hat{\nu}, \; \tilde{\boldsymbol{r}}_i = \boldsymbol{r}_i + \frac{\kappa}{100}\hat{\eta} \tag{43}$$

where κ denotes the initial offset magnitude and $\hat{\nu}, \hat{\eta}$ are unit-norm vectors with randomly drawn components. These nearby reference orbits are then propagated forward in time and provided as nominal states for two I-KFs: one which includes the absolute δ_i states, and one which assumes that these states are known perfectly (i.e., that $\tilde{r}_i = r_i$). This model is primarily pedagogical, but reflects scenarios in which an inaccurate nominal orbit is available from other ground- or space-based sources. An example of such a scenario is the use of Two-Line Element Sets as an on-board ephemeris, which is a common practice among cubesat groups which lack native orbit determination capabilities.

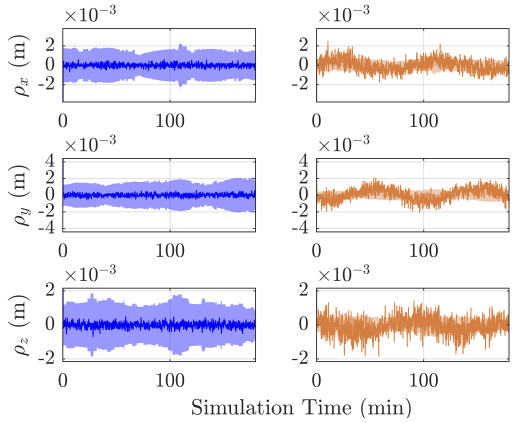

(a) Relative position estimate errors. Shaded areas represent the 2-σ covariance bounds for the estimate error.

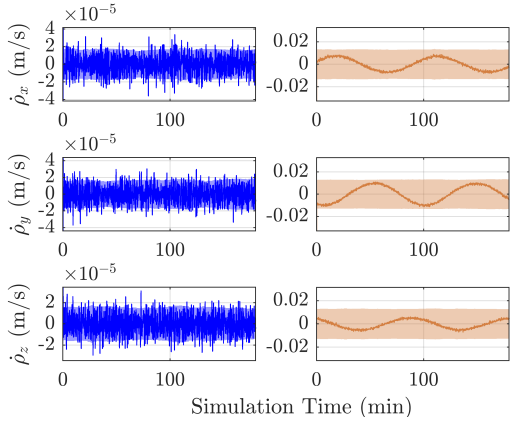

(b) I-KF (left, blue) and LL-KF (right, orange) velocity errors and 2-σ bounds for velocity error.

Figure 6: Comparison of incremental (blue, left) and leader-linearized filter (red, right) errors for ρ= 10,000m, λ=1,000 case. Shaded regions indicate 2-σ covariance bounds, which vary with the geometric dilution of precision (GDOP) and appearance/disappearance of GPS measurements for both filters. Note the improvement of performance by two orders of magnitude in the relative position states and three orders of magnitude in the velocity states.

The δ- states of the incremental architecture can be interpreted as directly attempting to correct this class of incorrect nominals. To demonstrate this, the filters of the previous section were run again with perturbed nominal information to varying degrees. The resulting RMS position error and RMS velocity errors were calculated for the final orbit of each scenario, shown in Figure 8.

At all points, the incremental architecture provides superior accuracy to the leader-linearized filter, and its performance is essentially invariant to mis-modeled absolute reference positions. This loss of accuracy is analogous to the long-baseline case demonstrated in Figure 4; in this case, the LL-KF becomes inconsistent due to ignoring the potential for errors on the absolute state and their coupling into the relative dynamics.

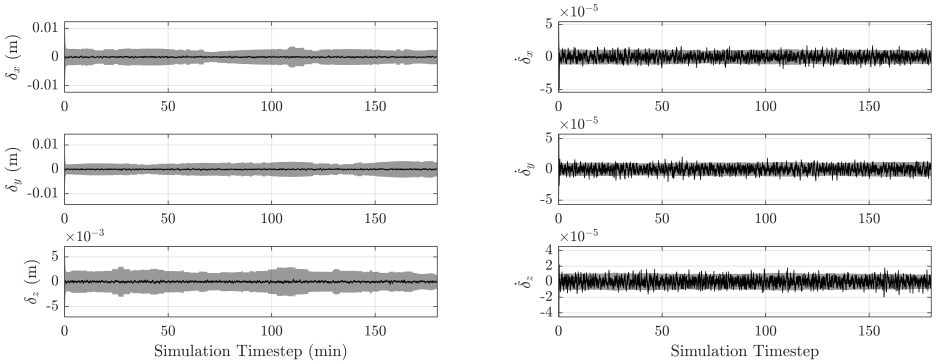

(a) EKF Position errors. Shaded areas represent the 1-σ covariance bounds for the estimate error.

(b) EKF Velocity errors. Shaded areas represent 1-σ bounds for velocity error.

Figure 7: Absolute δ errors over a simulation window for a baseline of 10,000m. Shaded areas represent 1-σ regions. Note that covariance bounds on the position and velocity are orders of magnitude larger than those for the relative states in Figure 6.

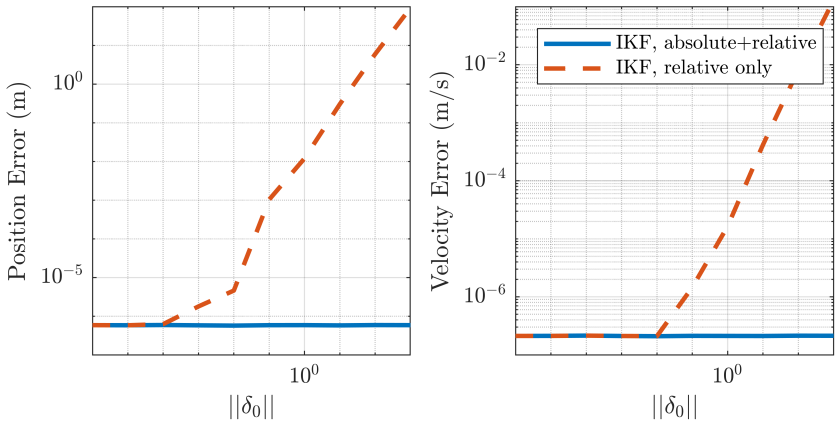

Figure 8: Variation of the LL-KF (red) and I-KF (blue) mean norm errors versus the magnitude of the nominal initial disturbance. Across all disturbance values, the I-KF outperforms the LL-KF.

SUMMARY AND CONCLUSION

The theory of "incremental" linearization for Kalman filtering is discussed to highlight its ability to accurately incorporate both absolute and relative measurements for improved numerics. The coupling of the absolute and relative dynamics was also shown to improve the relative estimation error. When only the relative state is considered, all uncertainty of the relative dynamics/measurement is forced onto the follower spacecraft. The dynamics coupling allows the uncertainty of the leader to be correlated to the relative state and also allows high-precision relative measurements to improve absolute state estimates. A second study analyzed the error associated with linearizing the dynamics and measurement equations across the entire formation was studied. Leader-linearized systems have similar *position* estimation performance with respect to self-linearized systems up to $\sim$1km separation distances. However, the relative *velocity* estimates are significantly degraded in all cases

which can drastically increase fuel usage.

ACKNOWLEDGMENT

The research described in this article was carried out at the Jet Propulsion Laboratory, California Institute of Technology, under a contract with the National Aeronautics and Space Administration.

REFERENCES

[1] L. Breger, J. How, and A. Richards. Model predictive control of spacecraft formations with sensing noise. In *Proceedings of the American Control Conference*, volume 4, page 2385. Citeseer, 2005.

[2] F.D. Busse. *Precise formation-state estimation in low earth orbit using carrier differential GPS*. PhD thesis, Stanford University, Department of Aeronautics and Astronautics, 2003.

[3] F.D. Busse, J.P. How, and J. Simpson. Demonstration of adaptive extended Kalman filter for low earth orbit formation estimation using CDGPS. *Journal of the Institute of Navigation*, 50(2):79–93, 2003.

[4] N. Filipe, M. Kontitsis, and P. Tsiotras. Extended kalman filter for spacecraft pose estimation using dual quaternions. *Journal of Guidance, Control, and Dynamics*, 38(9):1625–1641, September 2015.

[5] A.H. Jazwinski. *Stochastic Processes and Filtering Theory*. Dover Publications, Inc., 1998.

[6] S. Leung and O. Montenbruck. Real-time navigation of formation-flying spacecraft using global-positioning-system measurements. *Journal of Guidance, Control, and Dynamics*, 28(2):226–235, Mar-Apr 2005.

[7] F.L. Markley. Attitude error representations for Kalman filtering. *Journal of Guidance, Control, and Dynamics*, 26(2):311–317, Mar-Apr 2003.

[8] O. Montenbruck, S. D'Amico, J.-S. Ardaens, and M. Wermuth. Carrier phase differential GPS for LEO formation flying the PRISMA and TANDEM-X flight experience. In *Proceedings of the American Astronomical Society*, pages 1–20, 2010.

[9] M.L. Psiaki. Autonomous orbit determination for two spacecraft from relative position measurements. *Journal of Guidance, Control, and Dynamics*, 22(2):305–312, March-April 1999.

[10] B. Razgus, E. Mooij, and D. Choukroun. Relative navigation in asteroid missions using dual quaternion filtering. *Journal of Guidance, Control, and Dynamics*, 40(9):2151–2166, September 2017.

[11] Daniel P Scharf, Fred Y Hadaegh, and Scott R Ploen. A survey of spacecraft formation flying guidance and control (part ii): Control. 2004.

[12] L. Shu, P. Chen, X. Sun, and C. Han. Stochastic modeling and variance component estimation to GPS observables for LEO relative navigation applications. In *Proceedings of the AIAA GN&C Modeling and Simulation Technologies Conference*, pages 1–12, 2013.

[13] S.Mohiuddin and M.L.Psiaki. High-altitude satellite relative navigation using carrier-phase differential global positioning system techniques. *Journal of Guidance, Control, and Dynamics*, 30(5):1427–1436, Sep-Oct 2007.

[14] S.Mohiuddin and M.L.Psiaki. Carrier-phase differential global positioning system navigation filter for high-altitude spacecraft. *Journal of Guidance, Control, and Dynamics*, 31(3):801–814, Jul-Aug 2008.

[15] Y. Song and J.W. Grizzle. The extended kalman filter as a local asymptotic observer for nonlinear discrete-time systems. In *1992 American Control Conference*, pages 3365–3369, June 1992.

[16] Y. Xing, X. Cao, S. Zhang, H. Guo, and F. Wang. Relative position and attitude estimation for satellite formation with coupled translational and rotational dynamics. *Acta Astronautica*, 67:455–467, 2010.